

Hosting Ability of Mesoporous Micelle-Templated Silicas toward Organic Molecules of Different Polarity

Alberto Moscatelli,[†] Anne Galarneau,[‡] Francesco Di Renzo,[‡] and M. Francesca Ottaviani^{*,†}

Institute of Chemical Sciences, University of Urbino, Piazza Rinascimento 6, 61029 Urbino, Italy, and Laboratoire de Matériaux Catalytiques et Catalyse en Chimie Organique, UMR 5618 ENSCM-CNRS, 8 rue de l'Ecole Normale, 34296 Montpellier Cedex 5, France

Received: July 6, 2004; In Final Form: September 10, 2004

Spin probe water solutions were adsorbed onto differently treated micelle-templated silicas (MTS) of different pore sizes to analyze the hosting ability of the MTS surface toward different organic molecules. The MTS synthesis was performed at 388 K by self-assembly of inorganic silica and micelles of cetyltrimethylammonium bromide (CTAB) to which different amounts of 1,3,5 trimethylbenzene (TMB) were added at different TMB/CTAB ratios to modify the pore size: 40, 65, and 80 Å pore diameter were obtained for TMB/CTAB ratio = 0, 2.7, and 13, respectively. As-synthesized MTS, calcined MTS, and octyldimethyl(C8) grafted MTS were used. These MTS were characterized by means of nitrogen sorption isotherms and TEM as homoporous silica with regular and reproducible structure. Different spin probes (nitroxides) were taken as models for different types of organic molecules, namely, neutral and charged molecules and surfactants. The computer aided analysis of the electron paramagnetic resonance (EPR) spectra of these probes provided information on the hosting ability of the differently treated solid surface in respect of the different structure and hydrophilicity of the probes. The spectral analysis allowed the depiction of the probable distribution and location of the different probes at the differently treated silica surfaces. For the as-synthesized MTS, void space became available for the probe adsorption in vicinity of the surface when TMB was used in the synthesis and then evaporated. For the calcined MTSs, the hydrophobic sites at the solid surface, namely, siloxanes, increased by increasing the TMB content in the synthesis mixture. The binding of the EPR probe with the surface of these MTS is favored when both hydrophilic and hydrophobic interactions occur, as found with surfactant probes bearing both a hydrophilic and a hydrophobic moiety. For the C8-grafted MTSs, the results provided a proof of the quality of grafting: the surface is largely hydrophobic and favors self-aggregation of the surfactant probes, led by chain–chain interactions.

Introduction

Micelle-templated silica (MTS) materials,^{1–6} obtained by a cooperative assembly of micelles and silicates, have a high potential for applications in several fields of physical chemistry, such as catalysis, adsorption, and host–guest chemistry,^{7–13} because of uniform pore sizes between 20 and 150 Å. The formation mechanism of the hexagonal MTS in basic media can be followed by different techniques.^{14–23} Among these different techniques, electron paramagnetic resonance (EPR) of probes dissolved in the micelles already demonstrated to provide in situ information about MTS synthesis.^{24–28} In a previous study,²⁸ we followed the synthesis of MTS by means of an EPR probe, 4-cetyltrimethylammonium-2,2,6,6-tetramethyl-piperidine-1-oxyl bromide (CAT16), embedded in cetyltrimethylammonium bromide (CTAB) micelles to whom different amounts of 1,3,5-trimethylbenzene (TMB) were added to increase the pore size. The results indicated that the formation of hydrophilic and hydrophobic sites at the solid surface is due to the localization of TMB in the vicinity of the polar heads of the surfactants.

EPR has revealed itself to be a very useful tool to analyze the surface properties of silica-based particles, by means of spin

probes that interact differently with the surface sites, as a function of their structure (size and shape), polarity, and charge.^{29,30} These previous studies have shown how the silanol groups of the silica surface play a substantial role in binding polar and charged probes, which also monitor the variation of the rheological properties of the adsorbed solvent.

Therefore, to analyze the surface properties of the MTS obtained with different TMB/CTAB ratios, various nitroxide radicals (Scheme 1), differing in structure, polarity, and charge, were adsorbed from water solutions at the surface of the solids in different experimental conditions. The selected nitroxide radicals were the following:

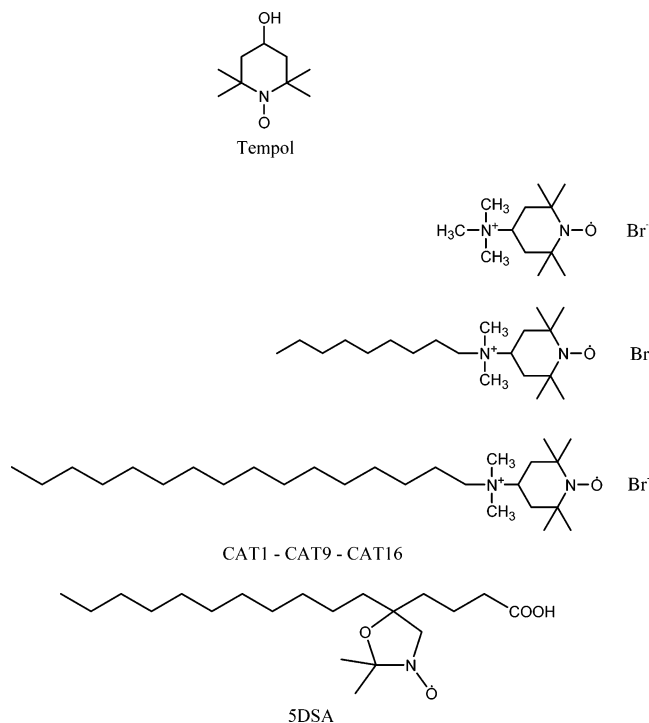
- 4-hydroxyl-2,2,6,6-tetramethylpiperidine *N*-oxide (Tempol): used as small organic molecule bearing both low polar and polar functions
- 4-trimethylammonium-2,2,6,6-tetramethylpiperidine *N*-oxide bromure (CAT1)
- 4-nonyl, dimethylammonium-2,2,6,6-tetramethylpiperidine *N*-oxide bromure (CAT9)
- 4-cetyl, dimethylammonium-2,2,6,6-tetramethylpiperidine *N*-oxide bromure (CAT16)
- 5-doxylstearic acid (5-DSA)

The computer-aided analysis of the EPR spectra allows the extraction of structural, mobility, and polarity information on the probes and their environments when adsorbed at different surface sites of MTS.

* Corresponding author. Email: ottaviani@uniurb.it; tel: +39-0722-4164; fax: +39-0722-2754.

[†] University of Urbino.

[‡] Laboratoire de Matériaux Catalytiques et Catalyse en Chimie Organique.

SCHEME 1: Formulas of the Spin Probes Used for Surface Characterization

The solids used for the surface characterization were synthesized at 388 K, which allowed us to obtain homoporous hexagonal MTS with pore sizes of about 40, 65, and 80 Å for TMB/CTAB ratio = 0, 2.7, and 13, respectively.

To provide an overall view of the system under study, we have studied the surface properties of MTS in three different conditions: (a) as-synthesized, that is, still containing the original surfactant aggregates in the structure framework; (b) calcined, that is, after high-temperature treatment that eliminates the organic matter inside the pores; (c) grafted, that is, upon functionalization of the silanol groups with octyl chains: this process renders hydrophobic the surface. These different MTS were also characterized by nitrogen adsorption isotherms and transmission electron microscopy (TEM). Unfortunately, X-ray diffraction (XRD) patterns did not provide any informative pattern for the MTS synthesized in the presence of TMB, due to the large pore size.

Experimental Procedures

Materials. MTS Synthesis. The components were added in the following sequence:

Water (Millipore)	molar ratio	20
CTAB (Sigma-Aldrich)	molar ratio	0.1
NaOH (Sigma-Aldrich)	molar ratio	0.25
TMB (Sigma-Aldrich)	molar ratio	0–0.27–1.3
SiO ₂ (Lichrosphere 100-Merck)	molar ratio	1

The resultant slurry was stirred for 30 min at room temperature and put in autoclave at 388 K for 24 h, for the synthesis in the absence of TMB; for the synthesis with TMB, 1 h was enough to obtain the final MTS, which were then filtered and washed with water until a neutral pH was obtained. Mass spectrometry of the filtered water indicated that only negligible amounts of TMB and CTAB were lost in the filtration procedure. Finally, the obtained MTS were dried at 353 K. These MTS were analyzed as-synthesized: they contain the surfactants,

but all TMB was removed during the drying process. Calcination has been performed at 823 K for 8 h. The grafted-MTS have been obtained from anhydrous calcined MTS by adding to MTS chlorodimethyloctylsilane corresponding at 5 grafting agent/nm² of MTS and pyridine (1 pyridine/grafting agent) in refluxing toluene. The reagents were stirred for 15 h before filtration and then washed. The samples were dried at 353 K overnight. MTS have been characterized by thermogravimetric analysis, by nitrogen sorption isotherm and by TEM.

EPR Samples. Portions of 1 mL of 1 mM solutions of CAT1, CAT9, CAT16, (kindly provided by Dr. X. Lei, Columbia University, New York), and Tempol (Sigma-Aldrich, used as received) in Millipore doubly distilled water were added to vials containing 250 mg of solid. 5DSA (Sigma-Aldrich, used as received) was dissolved in chloroform (Merck) at concentration of 1 mM. A total of 1 mL of this solution was transferred in a vial, and the solvent was evaporated. A total of 1 mL of Millipore water was added to this vial, and the solid was then added under stirring. Various solid–solution mixtures were left equilibrating for various periods of time (from 1 h to 1 week) in sealed vials in dark conditions at room temperature under gentle stirring. Then the vials were left separating the liquid from the solid until the supernatant solution separated from the solid. The supernatant solution after adsorption was analyzed and compared to the unadsorbed solution to determine the adsorbed amounts of radicals. The solid was gently dried on a filter paper until the original dry consistency was obtained. In this way, the adsorbed solution, retained in the internal cavities of the solid, was only analyzed.

Different adsorption times changed the adsorption percentages: for the calcined MTS, the adsorption percentage increased in the first 5 h, after that it remained constant for about 2 days, and then it decreased in a not reproducible way (results not shown). The spectra of the solids after adsorption also changed accordingly (results also not shown). We interpreted these findings as follows: 5 h are needed as equilibration time to complete the adsorption process, then the calcined MTS structure remained stable for 2 days before collapsing due to hydrolysis. The stability of the mixture decreases with the increase of the amount of water and of the stirring speed. For the grafted and as-synthesized materials, the stability results longer (about 3 and 4 days, respectively), as indicated by the reproducibility of the EPR results. Henceforth, the EPR results were analyzed after 1 day equilibration of the solid with the probe solution.

The stability of the radicals over the time of the EPR analysis was ensured by the constant intensity of the experimental EPR spectra.

Methods. EPR spectra were recorded by means of an EMX-Bruker spectrometer operating at the X band (9.5 GHz). The temperature was controlled with a Bruker ST3000 variable-temperature assembly cooled with liquid nitrogen. The samples were inserted in glass tubes of 2 mm diameter. The adsorbed amount of radicals was measured on the basis of the intensity decrease of the EPR signal from the unadsorbed radical solution to the supernatant solution after adsorption by means of a flat cell fixed in the EPR cavity.

Nitrogen sorption isotherms were performed at 77 K on Micromeretic ASAP 2010 instrument after being outgassed at 523 and 423 K for calcined MTS and as-synthesized and grafted MTS, respectively.

Transmission electron microscopy (TEM) was performed using a Philips CM30T electron microscope with an LaB6 filament at 300 kV. Samples were mounted on a microgrid carbon polymer supported by a copper grid. A few droplets of

a suspension of ground sample in ethanol were dropped on the grid and then dried at ambient conditions.

EPR Computation. The analysis of the EPR spectra was carried out by means of the simulation program by Freed and Budil et al.,³¹ which takes into account the relaxation process and therefore allows us to correctly compute the EPR line shape: the main parameters extracted from the spectral analysis are (a) the coupling tensor between the electron spin and the nuclear spin, \mathbf{A} , mainly the A_{zz} component, whose increase is related to an increase in environmental polarity of the radicals; (b) the correlation time for the rotational motion of the probe, τ_c : the Brownian diffusion ($D_i = 1/(6\tau_i)$) or the Jump diffusion ($D_i = 1/\tau_i$) models are tried in the computation. In both cases, the main component of the correlation time for motion is the perpendicular one, τ_{\perp} ; (c) the intrinsic line width, ΔH , which increases with the increase of the spin–spin interactions (mainly dipolar), is due to labels sitting in close sites. In few cases, found for 5DSA, an order parameter, S , is also needed in the computation, which measures the wobbling mobility of the surfactants in an ordered structure, due to the arrangement of the surfactants in a bilayerlike structure.

In most cases, the spectra are constituted by different components, and the analysis needed a subtraction–addition procedure of the components to provide the relative percentages (by double integration of the correspondent signals), corresponding to probes localized in different environments, that is, at different interacting sites of the solid surface. Each component could be extracted by subtraction of experimental spectra in which two components contributed in different percentages with respect to each other. Also, each component was computed and then subtracted from the experimental spectra to extract the other components. Finally, the computed components were added to each other at the right percentages to fit the experimental line shape.

The accuracy of the parameters (5%) was determined by computation: a variation of a parameter larger than 5% led to a perceptible variation of the computed line shape, and consequently, to a worst fitting between the computed and the experimental spectrum.

Of course, different sets of parameters could provide an equivalent or even better fitting between the experimental and the computed line shapes; but from several attempts of computations, the ones reported in this study are the most confident for the physical meaning of the systems; we mainly trusted the trends of the parameters in a series of EPR measurements on similar systems.

Results and Discussion

Properties of MTS from Nitrogen Sorption Isotherms and TEM. Figure 1 shows the nitrogen sorption isotherms at 77 K of the MTS synthesized with TMB/CTAB = 0, 2.7, and 13 at 388 K and then calcined. The isotherms are of type IV (IUPAC classification), showing well-defined cylindrical pores at increasing pore size with the increase in TMB/CTAB; the pore filling pressure increases with the increase in TMB. Similarly, nitrogen sorption isotherms were performed for the as-synthesized and C8-grafted MTS obtained with TMB/CTAB = 0, 2.7, and 13. The surface parameters characterizing the materials are reported in Table 1: pore volume = V , pore diameter = D_{BdB} (diameter according to Broekhof and De Boer)³², and BET surface area = S_{BET} are directly obtained from the nitrogen isotherm. S^* is the corrected surface area (by a 13.5 \AA^2 per sorbed nitrogen instead of 16.2 \AA^2) for hydroxylated surface.³² Org/nm²* represents the density of surfactant or octyl

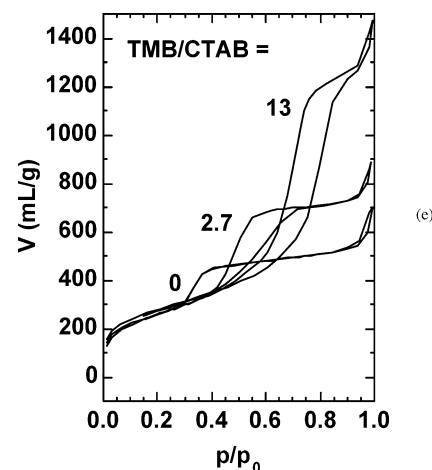


Figure 1. Nitrogen adsorption–desorption isotherms, obtained for MTS synthesized at 388 K and then calcined: TMB/CTAB = 0, 2.7, 13.

TABLE 1: Properties of MTS Synthesized at 388 K with Different TMB/CTAB Ratios under Different Forms: As-Synthesized, Calcined, and Grafted with Dimethyloctyl Chains^a

TMB/CTAB– samples	V (mL/g)	D_{BdB} (Å)	S_{BET} (m ² /g)	S^* (m ² /g)	org/nm ² *
0–as-syn	nonporous	nonporous	144		1.68
2.7–as-syn	0.81	55	430		1.51
13–as-syn	0.95	69	406		1.33
0–calc	0.79	39	979	816	
2.7–calc	1.47	65	884	737	
13–calc	1.67	79	857	714	
0–graft	0.29	26	ind. ^b		1.66
2.7–graft	0.98	55	608		1.52
13–graft	1.05	66	517		1.50

^a Pore volume (V), pore diameter (D_{BdB}), and BET surface area (S_{BET}) are directly obtained from the nitrogen isotherm. S^* is the corrected surface area (by a 13.5 \AA^2 per sorbed nitrogen instead of 16.2 \AA^2) for hydroxylated surface. Org/nm²* represents the density of surfactant or of octyl chains, calculated with the correction of surface area and TGA.

^b Ind. pore sizes are too small to correctly evaluate the BET surface area.

chains per surface of calcined material, calculated with the correction of surface area and TGA.

The calcined MTS used for adsorption have diameters of about 40, 65, and 80 Å for TMB/CTAB ratio = 0, 2.7, and 13, respectively. Grafted and as-synthesized MTS have porous space available for nitrogen sorption, except for the as-synthesized MTS obtained without TMB. The density of surfactant in the as-synthesized MTS decreases from 1.7 surfactants/nm², for TMB/CTAB = 0, to 1.5 surfactants/nm², for TMB/CTAB = 13. This corresponds to one surfactant in a surface of 8.7 and 9.8 Å diameter for MTS synthesized with TMB/CTAB = 0 and TMB/CTAB = 13, respectively. Therefore, the use of TMB in MTS synthesis leads to a low packed assembly of surfactants, which is a proof of the swelling role of TMB. Grafted-MTS shows a similar behavior: the octyl chains are low packed on MTS synthesized with TMB. We found that the density of grafted chains is equivalent to the density of surfactants. Therefore, the octyl chains attached in the surface zone where the surfactants localized before calcination.

Figure 2 shows the TEM images of the calcined MTS obtained for TMB/CTAB = 2.7 and 13. As it results from the TEM images, these MTS are characterized by homogeneous hexagonal pores.

Characterization of the Hosting Ability of MTS Surface from EPR. For each radical and each MTS, EPR spectra were

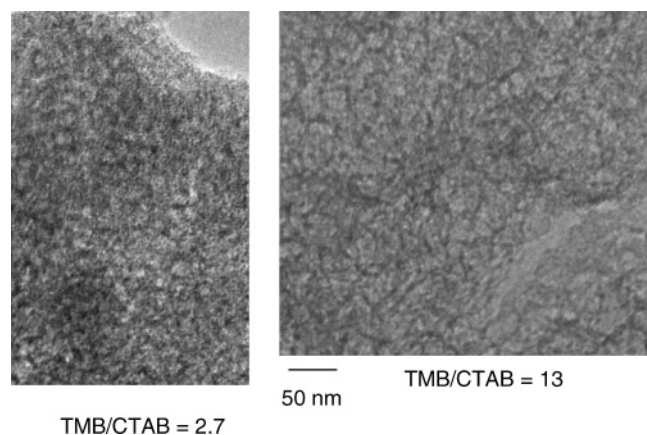


Figure 2. Transition electron micrographs (TEM) of MTS synthesized at 388 K with TMB/CTAB = 2.7 and 13.

recorded for the solid (gently dried onto a filter paper to remove the external probe solution) after adsorption, for the unadsorbed solution before adsorption, and for the supernatant solution after adsorption. The intensity decrease from the unadsorbed to the supernatant solution provided the percentage of adsorbed probe.

The spectra of the solids were analyzed by computation to extract the parameters that describe the interactions of the probes with the surface sites. Figure 3 shows examples of the EPR spectra (experimental: full lines; computed: dashed lines) recorded at 298 K for CAT1 and CAT16 adsorbed onto calcined MTS, whereas Figure 4 shows examples of the EPR spectra (experimental: full lines; computed: dashed lines) recorded at 298 K for Tempol and 5DSA adsorbed onto calcined MTS. The spectra for all MTS—calcined, grafted, and as-synthesized, obtained with different TMB/CTAB amounts—are constituted by different components that were separated by a subtraction procedure and then computed. The main parameters used for computation (A_{zz} , increasing with the increase in the environmental polarity; τ_{perp} , increasing with the increase in the strength of interaction; and ΔH , increasing with the increase of the local concentration of probes) are reported for each radical in Table 2. On the basis of these parameters, the spectral components were identified as follows:

(i) weakly interacting component, termed weak component (to be compared with the strong component, see the following), which is due to radicals characterized by a correlation time for motion between fast and slow motion conditions, that is,

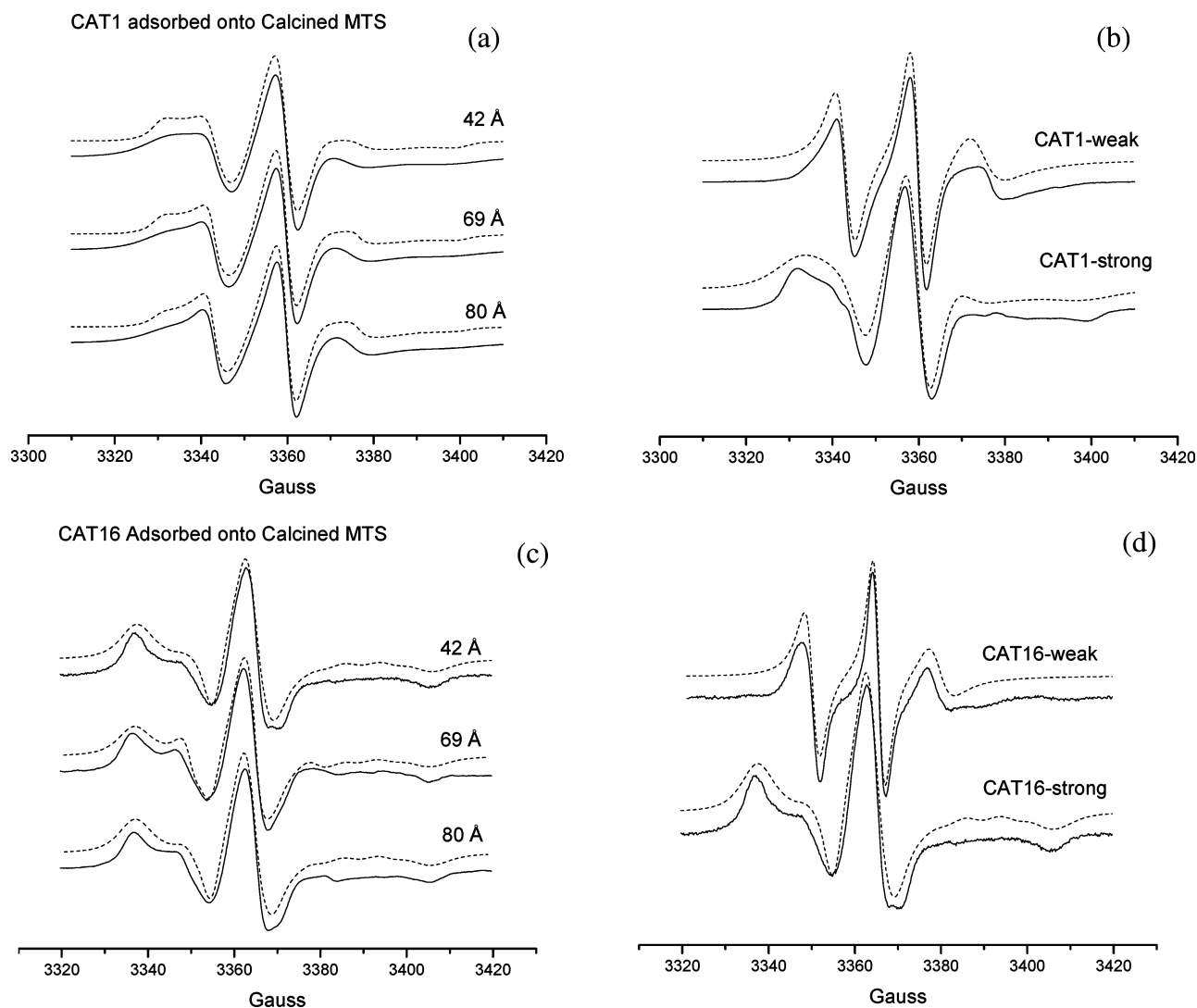


Figure 3. EPR spectra at 298 K of CAT1 (a) and CAT16 (c) adsorbed onto the calcined MTS with different pore sizes (different amounts of TMB in the micelles). The weakly interacting (weak) and strongly interacting (strong) components of the spectra obtained from a subtraction procedure of the experimental signals are reported for CAT1 (b) and CAT16 (d). Full lines: experimental spectra; dashed lines: computed spectra (the main parameters used for the computation of the components are reported in Table 2). The computations in Figure 1a,c are obtained by adding the computed components at the proper relative intensities to reproduce the experimental line shapes.

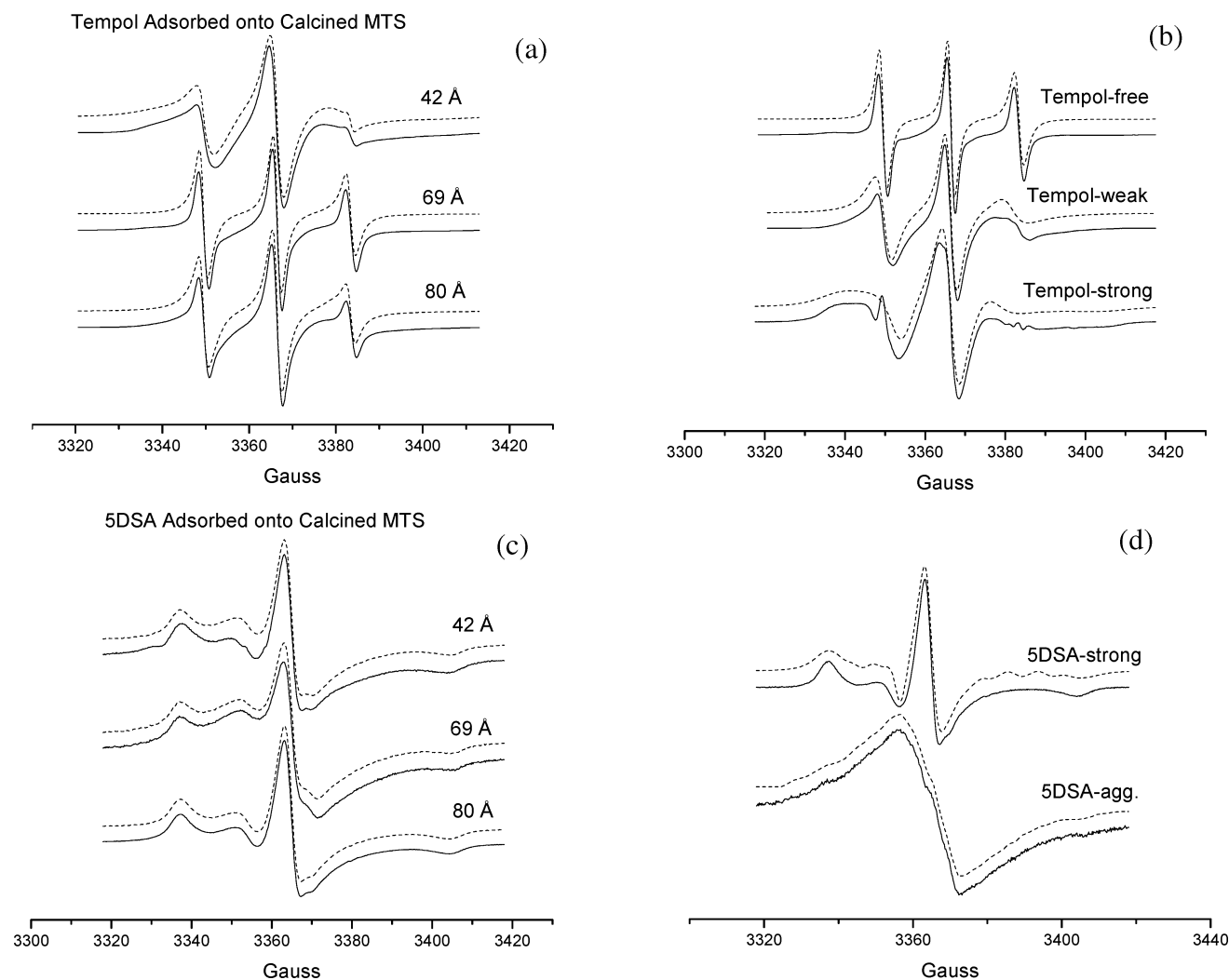


Figure 4. EPR spectra at 298 K of Tempol (a) and 5DSA (c) adsorbed onto the calcined MTS with different pore sizes (different amount of TMB in the micelles). The free (free), weakly interacting (weak), strongly interacting (strong), and aggregated (agg) components of the spectra, obtained from a subtraction procedure of the experimental signals, are reported, if present, for Tempol (b) and 5DSA (d). Full lines: experimental spectra; dashed lines: computed spectra (the main parameters used for the computation of the components are reported in Table 2). The computations in Figure 1a,c are obtained by adding the computed components at the proper relative intensities to reproduce the experimental line shapes.

TABLE 2: Main Parameters (Accuracy 5%) Obtained from Simulations of the Different Components for CATn Probes Adsorbed onto MTS^a

comp.	A_{zz} (G) CAT1	τ_{perp} (s) CAT1	ΔH (G) CAT1	A_{zz} (G) CAT9	τ_{perp} (s) CAT9	ΔH (G) CAT9	A_{zz} (G) CAT16	τ_{perp} (s) CAT16	ΔH (G) CAT16
free	36	3×10^{-11}	1.0	37.5	5×10^{-11}	1.0	35	7×10^{-11}	1.0
weak	36	2.5×10^{-9}	1.0				36.5	1×10^{-9}	0.5
strong	38.5	5.5×10^{-9}	1.5	37–36	8×10^{-9}	3–6	36	9×10^{-9}	4.0
agg							36	3×10^{-9}	8.0

comp.	A_{zz} (G) Tempol	τ_{perp} (s) Tempol	ΔH (G) Tempol	A_{zz} (G) 5DSA	τ_{perp} (s) 5DSA	ΔH (G) 5DSA	S 5DSA
free	37.5	1.5×10^{-11}	1.0				
weak	37	2×10^{-9}	1.5	34	2×10^{-9}	1.0	0.4
strong	37	5×10^{-9}	0.5	36	9×10^{-9}	0.5	
agg				35	2×10^{-9}	8.0	

^a Accuracy of the parameters from computation: 5%.

$\tau_{\text{perp}} = (1-3) \times 10^{-9}$ s. These conditions are accounted by weak interactions between the radicals and the surface interacting sites, such as radicals inserted in aggregates (micelles or a bilayerlike structure) of other surfactants or dipolarly interacting with the surface. The weak component is absent for CAT9 since this radical strongly interacts with the surface sites. The mobility of this weak component is comparable for all probes, being a little bit higher for CAT16 (the chain perturbs the interaction

of the head) and a little bit lower for CAT1 (no chain perturbation). The environmental polarity of weakly interacting probes is lower for 5DSA than for the other probes, due to the hydrophobic character of 5DSA.

(ii) Strongly interacting component, termed strong component, which arises from radicals characterized by a correlation time for motion matching the so-called slow motion conditions ($\tau_{\text{perp}} = (5-9) \times 10^{-9}$ s). These conditions are due to radicals

interacting with polar surface sites or trapped in a restricted space and binding hydrophilic and hydrophobic sites. The strong component is present for all probes. The mobility of the interacting probes decreases in the series Tempol > CAT1 > CAT9 > CAT16 = 5DSA; this indicates a synergic effect of the hydrophilic and hydrophobic interactions since the presence of the chain enhances these interactions. The longer the probe chain, the lower the environmental polarity of the strongly interacting probes is.

(iii) Free component, which is due to hydrated probes in fast-motion conditions since it does not interact with the surface or weakly interact with hydrophobic sites. The free component is absent for 5DSA since this radical is not water soluble. The mobility of the free probes decreases in the series Tempol > CAT1 > CAT9 > CAT16, which correlates well to the size of the radicals. Also, free CAT16 feels a lower environmental polarity since the long hydrophobic chain perturbs the nitroxide environment.

(iv) Aggregated component, termed agg component (the characterizing spectral parameter is the high line width, ΔH), which is due to condensation of the hydrophobic chains of the probes (for CAT16 and 5DSA) with the C8 chains of the grafted MTS. CAT16 probes showed a lower mobility ($\tau_{\text{perp}} = 6 \times 10^{-9}$ s) with respect to 5DSA ($\tau_{\text{perp}} = 2 \times 10^{-9}$ s) in the aggregates, due to the relatively strong interactions of the charged heads with the polar sites.

However, the different spectral components differently contribute to each EPR experimental spectrum. The analysis of the spectra by means of the subtraction procedure to extract each component, and the addition of the computed components to reproduce the experimental line shape (Figures 3 and 4), provided the percentages of each component for each probe adsorbed onto each MTS. These percentages are reported in form of histograms in the Figures 5–9 for the different probes: Figure 5: Tempol; Figure 6: CAT1; Figure 7: CAT9; Figure 8: CAT16; and Figure 9: 5DSA. In the figures, the percentages of the adsorbed probes, obtained from the intensity decrease from the unadsorbed solutions to the supernatant solutions, also are reported in form of histogram for each probe.

We analyze, compare, and discuss the results for each probe in each type of MTS (as-synthesized, calcined, and grafted), as follows.

Tempol. As-Synthesized. This small organic radical bearing an OH group is soluble both in more polar and in less polar environments; so, even in the condition of complete occupation of the polar surface groups by the CTAB heads, this probe may insert at the micelle–solid interface, mainly at the border between hydrophilic and hydrophobic sites. The increase in pore size promotes adsorption (Figure 5, adsorbed percentage histogram) and weak interactions (Figure 5, 2-D histogram), since a void space becomes available where TMB was localized before evaporation, also in the vicinity of the CTAB heads. The binding modes of Tempol in the as-synthesized MTS are described in Scheme 2(top).

Calcined. The adsorption follows the opposite trend as found in the as-synthesized MTS: the larger the MTS pore size, the lower the adsorption is (Figure 5, adsorbed percentage histogram). In this case, the larger the pores, the larger the void space is in the middle of the pores; therefore, a larger fraction of probes localized in this void space with the increase of the pore size. From the analysis of the solid samples (Figure 5, 2-D histogram), it resulted that the probes distribute at the polar surface sites (strongly interacting component), at the border of the polar and the low polar surface sites (weakly interacting component), and

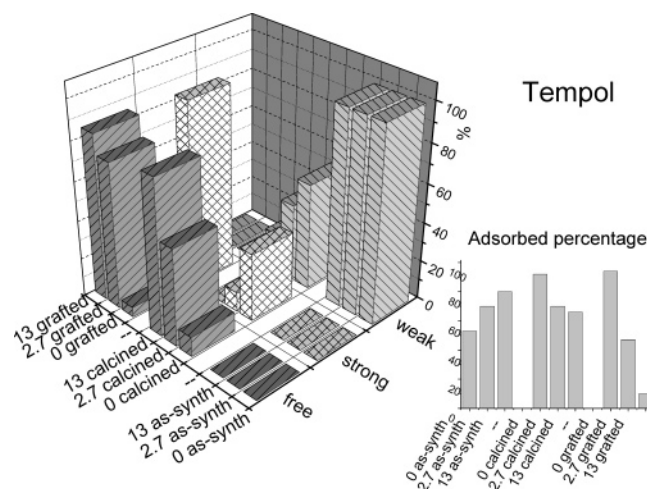
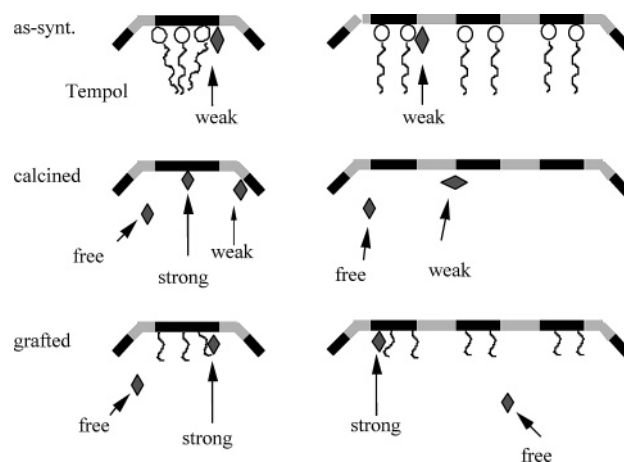


Figure 5. Adsorbed percentages (obtained from the EPR intensity decrease from the unadsorbed solutions to the supernatant solutions after adsorption) of Tempol in the different samples and different relative percentages of the spectral components (free, weakly interacting = weak, and strongly interacting = strong) for Tempol adsorbed onto the various solid samples.

SCHEME 2: Interactions of Tempol with the Different MTS^a



^a Black and gray bars represent hydrophilic and hydrophobic sites, respectively, on the MTS surface of pores.

in the water solution in the middle of the pores (free component) (the proposed location of the probes is described in Scheme 2 (middle)), but the relative amount of the free probes increases with the increase in pore size at the expense of the strongly and weakly interacting probes, as shown in Figure 5 (2-D histogram), due to the correspondent increase of free available volume.

Grafted. The probe is well-adsorbed into the small pore MTS, and then the adsorption decreases from small size to large size MTS (Figure 5, adsorbed percentage histogram), which is related to the increased available volume in the middle of the pores for the exchange between the surface and the unadsorbed solution. The contemporaneous hydrophilic–hydrophobic character of this probe prevails in favoring its adsorption at the surface of the hydrophobic grafted material leading to a strongly interacting component. (Figure 5, 2-D histogram). We propose that the interacting probes localized at the border between the grafted area and the low polar area, also interacting with the C8 chains, as described in Scheme 2 (bottom): in the small pores, the probes are constrained in a restricted space, whereas in the large pores, void space is available for the solution.

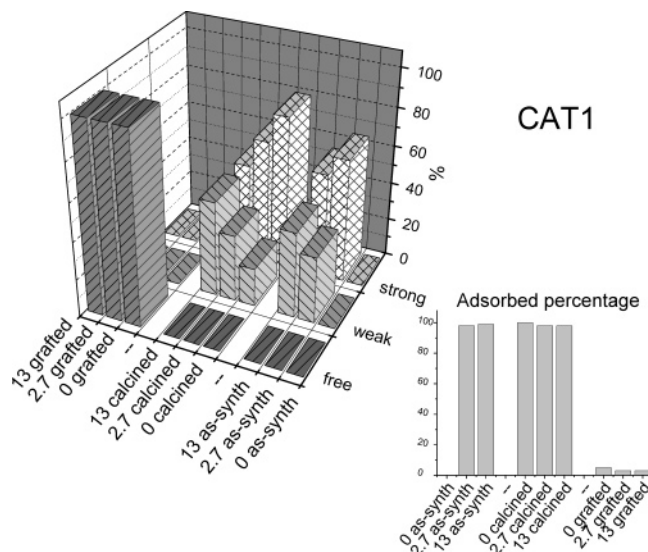
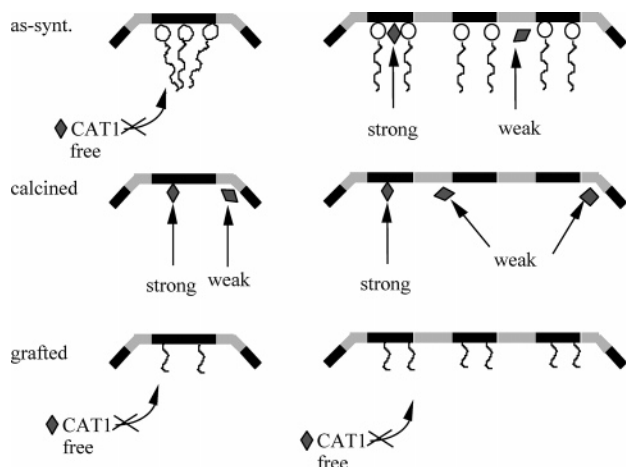


Figure 6. Adsorbed percentages (obtained from the EPR intensity decrease from the unadsorbed solutions to the supernatant solutions after adsorption) of CAT1 in the different samples and different relative percentages of the spectral components (free, weakly interacting = weak, and strongly interacting = strong) for CAT1 adsorbed onto the various solid samples.

SCHEME 3: Interactions of CAT1 with the Different MTS^a



^a Black and gray bars represent hydrophilic and hydrophobic sites, respectively, on the MTS surface of pores.

CAT1. As-Synthesized. The adsorption capability toward CAT1 is largely different with respect to Tempol since the charged CAT1 is only attracted by the polar surface sites. Therefore, the percentage of adsorbed solution, shown in Figure 6 (adsorbed percentage histogram), is zero in the small pores, where no free space is available for this charged probe, whereas it is high in the large pores (TMB/CTAB = 2.7 and 13 in the synthesis) where void space is available after TMB evaporation in the vicinity of the polar surface groups. In these large pore MTS, CAT1 competes with the CTAB heads for the interaction with the polar surface groups (silanols), giving rise to strongly interacting probes (Figure 6, 2-D histogram). Weakly interacting probes are also present (Figure 6, 2-D histogram), characterized by a low polar environment (Table 2); these probes are therefore located at less hydrophilic sites (siloxanes), originated by TMB in the synthesis process. The proposed adsorption modes of CAT1 onto as-synthesized MTS are depicted in Scheme 3 (top).

Calcined. The adsorbed percentage of probes shown in Figure 6 (adsorbed percentage histogram) is high. In this case, a large

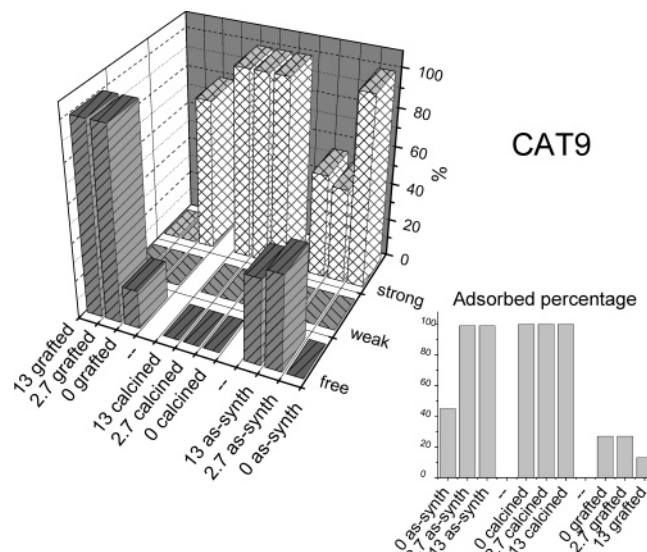
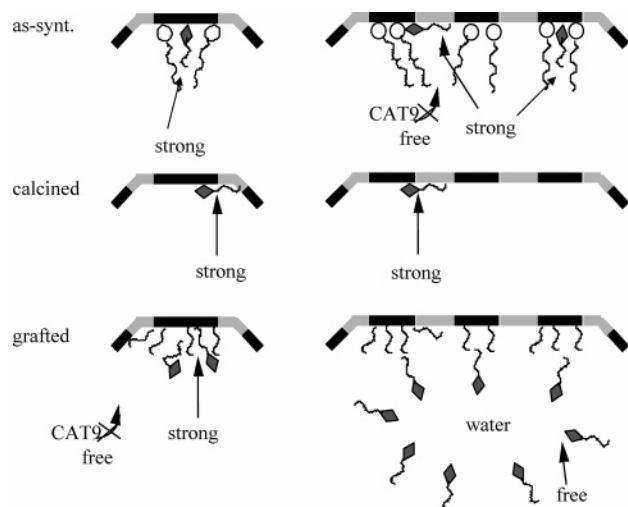


Figure 7. Adsorbed percentages (obtained from the EPR intensity decrease from the unadsorbed solutions to the supernatant solutions after adsorption) of CAT9 in the different samples and different relative percentages of the spectral components (free, weakly interacting = weak, and strongly interacting = strong) for CAT9 adsorbed onto the various solid samples.

fraction of the adsorbed probes goes to strongly interact with the polar surface sites. However, the strongly interacting probes diminish with the increase in pore size (increase in TMB/CTAB in the synthesis) in favor of weakly interacting probes (Figure 6, 2-D histogram). This means that the calcined MTS surface becomes less interactive toward the positively charged organic probes when more TMB is used in the synthesis. Therefore, a less hydrophilic surface is obtained due to TMB. However, the free component found for Tempol is absent in the spectra of the charged CAT1. The binding mode proposed for CAT1 onto the calcined MTS is also sketched in Scheme 3 (middle).

Grafted. Opposite to the calcined MTS, the grafted MTS hosts Tempol much more and much better than CAT1 (compare the adsorption percentages in Figures 5 and 6). The adsorption of CAT1 in the grafted MTS is very low, and this adsorbed CAT1 remains free in the pores (only the free component contributes to the spectra, as shown in Figure 6, 2-D histogram), as depicted in Scheme 3 (bottom). This behavior is a good proof of the quality of grafting that renders the silica surface completely hydrophobic and therefore unable to host the positively charged CAT1 probes.

CAT9. As-Synthesized. If compared to CAT1, CAT9 is in part (45%) adsorbed into the small size MTS (Figure 7, adsorbed percentage histogram) since it inserts in the CTAB micelles. Therefore, it mainly gives rise to a strongly interacting component (Figure 7, 2-D histogram): the CAT9 head interacts with the polar sites, and the chain is inserted in the CTAB chains (Scheme 4, top left). When the pore size increases, the adsorption increases, but a fraction of probes remains free (Figure 7, 2-D histogram). The presence of a free component for CAT9 instead of a weak interacting component, found for CAT1, may be surprising, but it is well-explained if we consider that the adsorption mode of CAT9 in the strongly interacting sites may be in two ways, as depicted in Scheme 4, top right: (a) it inserts in the CTAB aggregates, as it does in the small pore MTS or (b) the head interacts with the polar surface sites, and the chain interacts with less polar surface sites (probes laying on the surface); in this way, some CAT9 radicals, hosted in the void spaces of the large pore MTS, are impeded to approach

SCHEME 4: Interactions of CAT9 with the Different MTS^a

^a Black and gray bars represent hydrophilic and hydrophobic sites, respectively, on the MTS surface of pores.

the surface sites: these sites are saturated by CAT9 and repulse the other probes that remain free in the solution occupying the void spaces.

Calcined. CAT9 is completely adsorbed at the surface of the calcined samples (Figure 7, adsorbed percentage histogram) and strongly interacts with the surface sites (Figure 7, 2-D histogram). The diffusional rotation mobility of the interacting CAT9 is lower than found for CAT1 (correlation times for the strong components in Table 2). In this case, as proposed in Scheme 4 (middle), not only hydrophilic (ion–dipole) interactions link the radicals to the polar surface groups, but contemporaneous hydrophobic interactions of the CAT9 chains with the low polar surface sites (siloxanes) enhance the binding strength of the radicals with the silica surface.

Grafted. The adsorption of CAT9 in the grafted MTS is quite low (Figure 7, adsorbed percentage histogram), but higher than CAT1 due to the presence of the C9 chain. In the small pores, CAT9 is in part confined in a restricted space where the chain inserts in the C8 chains at the surface. The resulting signal is the strongly interacting one (Figure 7, 2-D histogram) characterized by a decrease in A_{zz} (from 37 to 36 G), due to the decreased environmental polarity, and an increase in line width (from 3 to 6 G), due to the vicinity of the probes (these variations of parameters are shown in Table 2). In the large pore MTS, the available space increases, and the probes gain in freedom of motion: only the free component is recorded (Figure 7, 2-D histogram). The proposed adsorption mode is described in Scheme 4 (bottom).

CAT16. As-Synthesized. CAT16 is largely adsorbed into both small and large pores (Figure 8, adsorbed percentage histogram) since it well inserts in the CTAB micelles. As found for CAT9, only the strongly interacting component is found in the small pores (Figure 8, 2-D histogram) since the CAT16 heads interact with the polar surface groups, whereas the CAT16 chains are inserted in the CTAB micelles. However, the adsorption mode changes in the large pore MTS for CAT16 with respect to CAT9: instead of the free component, the weak interacting component was found to contribute to the spectrum together with the strongly interacting component (Figure 8, 2-D histogram). In this case, both hydrophobic interactions of CAT16 chains with low polar surface sites and the large size of CAT16 favor a slow mobility of this probe, hosted in the void spaces

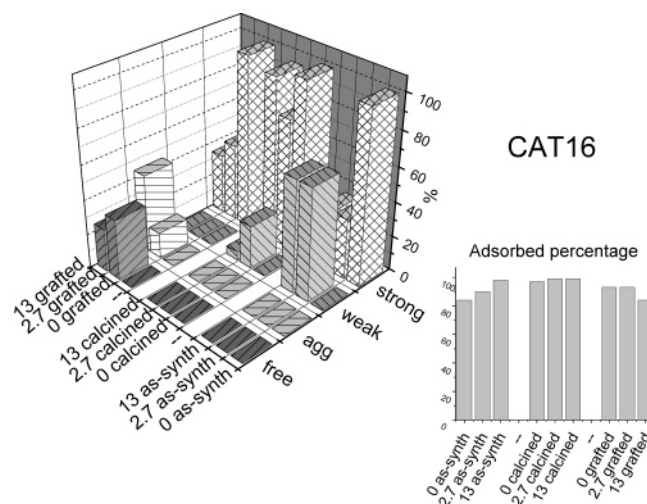
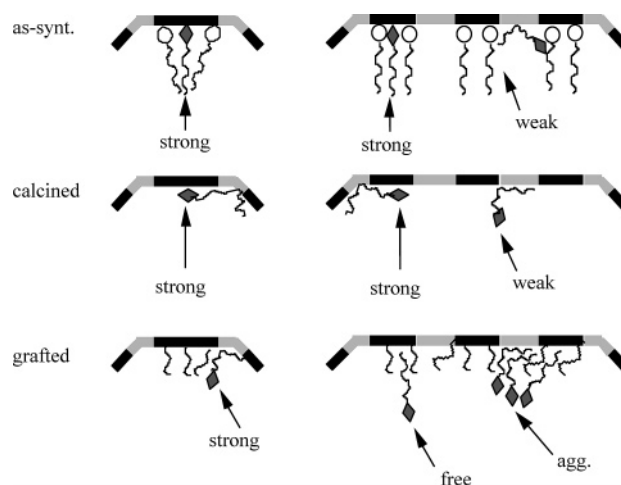


Figure 8. Adsorbed percentages (obtained from the EPR intensity decrease from the unadsorbed solutions to the supernatant solutions after adsorption) of CAT16 in the different samples and different relative percentages of the spectral components (free, weakly interacting = weak, strongly interacting = strong, and aggregated = agg) for CAT16 adsorbed onto the various solid samples.

SCHEME 5: Interactions of CAT16 with the Different MTS^a

^a Black and gray bars represent hydrophilic and hydrophobic sites, respectively, on the MTS surface of the pores.

created by TMB evaporation. The binding modes suggested for CAT16 in the as-synthesized MTS are depicted in Scheme 5 (top).

Calcined. The adsorption of CAT16 is quantitative in the calcined MTS (Figure 8, adsorbed percentage histogram). The behavior of CAT16 in the calcined samples is interesting: a weakly interacting component appears in the large pore MTS together with the strongly interacting component (Figure 8, 2-D histogram). We explain this behavior considering the binding mode described in Scheme 5 (middle): a part of radicals (strongly interacting) are able of anchoring both the head and the chain at the surface, with synergic hydrophilic and hydrophobic interactions, but the large size of CAT16 and the hydrophobicity of the radical chain prevents a fraction of the probe heads to easily approach the polar sites (only hydrophobic interactions may take place to minimize the chain/water repulsion), thus leading to a weakly interacting component.

Grafted. Different from the other CAT probes, CAT16 is well-adsorbed also into the grafted MTS (Figure 8: adsorbed percentage histogram) since the hydrophobic character of this

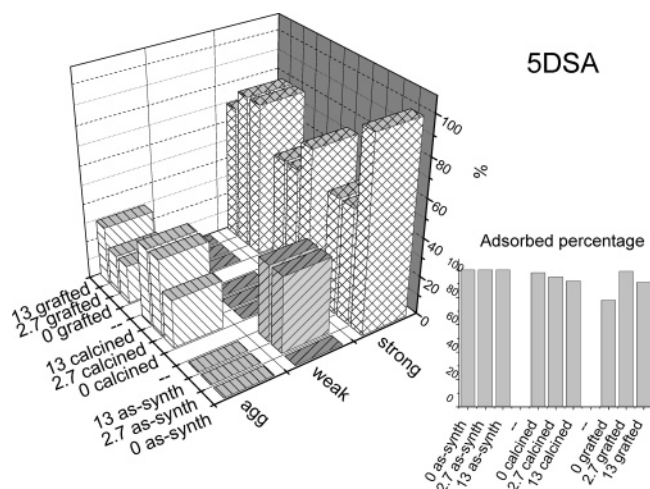


Figure 9. Adsorbed percentages (obtained from the EPR intensity decrease from the unadsorbed solutions to the supernatant solutions after adsorption) of 5DSA in the different samples and different relative percentages of the spectral components (free, weakly interacting = weak, strongly interacting = strong, and aggregated = agg) for 5DSA adsorbed onto the various solid samples.

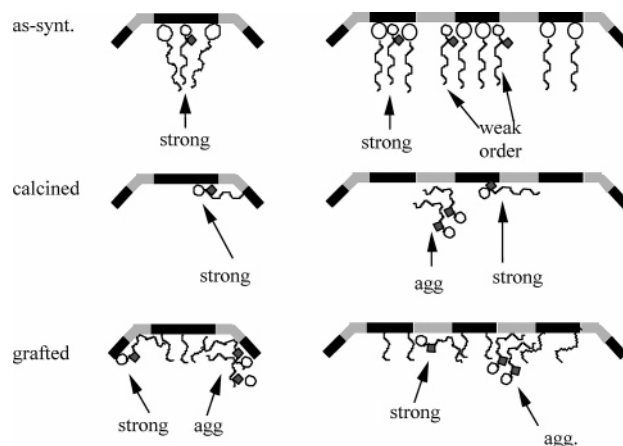
probe is high and is compatible with the hydrophobic character of the grafted MTS. In the small pores, only the strongly interacting component is present (Figure 8, 2-D histogram) since the radical is squeezed in the restricted pore space with the CAT16 chains well-anchored at the C8 surface chains (see Scheme 5, left bottom). In the large pores, both a free and an aggregated component come to contribute to the overall EPR signal (Figure 8, 2-D histogram). The aggregated component, which increases in relative intensity with the increase in the TMB/CTAB content in the synthesis, was computed with a quite large line width (8 G) and a slow motion condition ($\tau_{\text{perp}} = 6 \times 10^{-9}$ s), as reported in Table 2. Therefore, we propose the binding mode described in Scheme 5 (right bottom): the CAT16 chains aggregate at the surface, binding with both the C8 surface chains and the low polar surface sites formed by TMB in the synthesis.

5DSA. As-Synthesized. The adsorption of 5DSA is quantitative (Figure 9, adsorbed percentage histogram) since this probe well inserts in the CTAB aggregates. As for CAT16, a weakly interacting component superimposes to the strongly interacting one in the spectra of the large pore MTS (Figure 9, 2-D histogram), but the parameters used for computation in 5DSA spectra are different with respect to CAT16 (Table 2): a low polar environment and an order parameter characterize this weak interacting component. In this case, 5DSA is inserted in a monolayer of CTAB surfactants that are partially ordered at the MTS surface. Scheme 6 (top) shows the proposed location of 5DSA in the as-synthesized MTS.

Calcined. The adsorption of 5DSA is very high but not complete (Figure 9, adsorbed percentage histogram) since the polar surface is not so attractive toward the hydrophobic probes. The consequence is that a fraction of the probes self-aggregate (agg. component) to minimize the repulsion between 5DSA and the polar environment (Figure 9, 2-D histogram). The aggregation is favored in the large pore MTS, also because the low polar sites created by TMB during the synthesis offer a refuge to the hydrophobic probes. The model proposed for the interaction is described in the Scheme 6 (middle).

Grafted. Also in the grafted MTS, the adsorption is high (Figure 9, adsorbed percentage histogram), and a fraction of the probes forms aggregates (Figure 9, 2-D histogram), assisted by the C8 chains at the surface, whereas the other prevalent

SCHEME 6: Interactions of 5DSA with the Different MTS^a



^a Black and gray bars represent hydrophilic and hydrophobic sites, respectively, on the MTS surface of pores.

fraction is strongly interacting with the surface through hydrophilic and hydrophobic interactions with the surface sites (Scheme 6, bottom).

Definitely, the use of these probes provides a good picture of the hosting ability of the differently treated MTS toward the different probes. The contemporaneous availability of hydrophilic and hydrophobic interacting sites and their different distribution when different amounts of TMB are added to the synthesis mixture, the variation of the pore size, and the possibility to functionalize the surface render the MTS much more suitable than commercial silica to differentiate and select the adsorption of probe molecules as a function of charge, polarity, and size.

Conclusions

The computer-aided analysis of the EPR spectra obtained by adsorption of different typologies of radical probes from water solutions revealed the hosting ability of MTS, obtained by adding different amounts of TMB in the CTAB micelles used for MTS synthesis. The MTS were synthesized at 388 K from an inorganic silica source and characterized by means of nitrogen sorption isotherms and TEM. The increase in TMB allowed us to obtain well-defined sized pores with increasing pore size.

For the as-synthesized MTS, the analysis of the adsorbed probes provides not only a feature on the surface state of the materials but also complementary information on the synthesis process, concerning the structure of the micelles and the solids obtained at the end of synthesis. The surfactant aggregates are less packed when TMB is used in the synthesis and void spaces become available, after TMB evaporation, in the vicinity of the solid surface. Probe solutions are hosted in these spaces, and new hydrophobic surface sites (siloxane) are formed due to TMB in the synthesis mixture.

These low polar sites also play a substantial role in favoring the interactions of surfactant probes adsorbed inside the pores of the calcined MTS: the probe heads easily interact with the hydrophilic silanol groups at the surface, whereas the hydrophobic chains interact with the hydrophobic sites. Even hydrophobic probes such as the doxyl stearic acid strongly interact with the calcined MTS obtained with TMB. Therefore, it is noteworthy that the binding with the surface of large size MTS is favored when both hydrophilic and hydrophobic interactions occur.

The functionalization of the surface with C8 chains renders the surface completely hydrophobic and allows a surfactant molecule to form aggregated structures at the surface itself. These aggregates, therefore, are formed by cooperation of the probe chains, the octyl chains, and the hydrophobic surface sites, for the hydrophobic part, and by the water carried into the pores by the probe heads, for the hydrophilic part.

In summary, the hosting ability of the MTS surface, in the absence and in the presence of TMB in the synthesis, depends on the following factors:

- (i) the size of the pores
- (ii) the number and distribution of hydrophilic and hydrophobic interacting sites
- (iii) the functionalization of the surface
- (iv) physicochemical parameters, like temperature and hydration level

The use of surfactant probes not only helps in understanding the state of surface of the different MTS in terms of polarity and hydrophobicity, but these probes also mimic the interacting behavior of some polluting agents, which may be selectively extracted from the environment. In this respect, the probes used in this study were well-representative of different classes of polluting agents.

Acknowledgment. M.F.O. and A.M. thank the Italian Ministero dell' Università e della Ricerca Scientifica (MURST) and PRIN2002 for their financial support.

Supporting Information Available: Experimental and computed EPR spectra and components of CAT16 (a) and 5DSA (b) adsorbed onto as-synthesized, calcined, and grafted MTS obtained with TMB/CTAB = 13 as well as the main parameters used for computation. This material is available free of charge via the Internet at <http://pubs.acs.org>.

References and Notes

- (1) Kresge, C. T.; Leonowicz, M. E.; Roth, W. J.; Vartuli, J. C.; Beck, J. S. *Nature* **1992**, 359, 710.
- (2) Beck, J. S.; Vartuli, J. C.; Roth, W. L.; Leonowicz, M. E.; Kresge, C. T.; Schmidt, K. D.; Chu, C. T.-W.; Olson, D. H.; Sheppard, E. W.; McCullen, S. B.; Higgins, J. B.; Schenkler, J. L. *J. Am. Chem. Soc.* **1992**, 114, 10834.
- (3) Inagaki, S.; Fukushima, Y.; Kuroda, K. *J. Chem. Soc., Chem. Commun.* **1993**, 680.
- (4) (a) Huo, Q.; Margolese, D. I.; Ciesla, U.; Feng, P.; Gier, T. E.; Sieger, P.; Leon, R.; Petroff, P. M.; Schüth, F.; Stucky, G. D. *Nature* **1994**, 368, 317. (b) Huo, Q.; Margolese, D. I.; Ciesla, U.; Demuth, D. G.; Feng, P.; Gier, T. E.; Sieger, P.; Firouzi, A.; Chmelka, B. F.; Schüth, F.; Stucky, G. D. *Chem. Mater.* **1994**, 6, 1176.
- (5) Tanev, P. T.; Pinnavaia, T. J. *Science* **1995**, 271, 1267.
- (6) Bagshaw, S. A.; Prouzet, E.; Pinnavaia, T. J. *Science* **1995**, 269, 1242.

- (7) Armengol, E.; Cano, M. L.; Corma, A.; Garcia, H.; Navarro, M. Y. *J. Chem. Soc., Chem. Commun.* **1995**, 519.
- (8) (a) Corma, A.; Martinez, A.; Martinez-Soria, V.; Monton, J. B. *J. Catal.* **1995**, 153, 25. (b) Corma, A.; Navarro, M. T.; Pariente, J. P. *J. Chem. Soc., Chem. Commun.* **1994**, 147.
- (9) Tanev, P. T.; Chibwe, M.; Pinnavaia, T. J. *Nature* **1994**, 368, 321.
- (10) Wu, C. G.; Bein, T. *Science* **1994**, 264, 1757.
- (11) Llewellyn, P. L.; Ciesla, U.; Decher, H.; Stadler, R.; Schüth, F.; Unger, K. *Stud. Surf. Sci. Catal.* **1994**, 84, 2013.
- (12) Branton, P. J.; Hall, P. I. G.; Sing, K. S. W.; Reichert, H.; Schüth, F.; Unger, K. *J. Chem. Soc., Faraday Trans.* **1994**, 90, 2821.
- (13) Schmidt, R.; Stöcker, M.; Hansen, E.; Akporiaye, D.; Ellestad, O. H. *Microporous Mater.* **1995**, 3, 443.
- (14) Ying, J. Y.; Mehnert, C. P.; Wong, M. S. *Angew. Chem. Int. Ed.* **1999**, 38, 56.
- (15) Patarin, J.; Lebeau, B.; Zana, R. *Curr. Opin. Coll. Interface Sci.* **2002**, 7, 107.
- (16) (a) Chen, C. Y.; Li, H.-X.; Davis, M. E. *Microporous Mater.* **1993**, 2, 17. (b) Chen, C. Y.; Burkett, S. L.; Li, H.-X.; Davis, M. E. *Microporous Mater.* **1993**, 2, 27.
- (17) Vartuli, J. C.; Schmidt, K. D.; Kresge, C. T.; Roth, W. J.; Leonowicz, M. E.; McCullen, S. B.; Hellring, S. D.; Beck, J. S.; Schenkler, J. L.; Olson, D. H.; Sheppard, E. W. *Chem. Mater.* **1994**, 6, 2317.
- (18) Fyfe, C. A.; Fu, G. J. *Am. Chem. Soc.* **1995**, 117, 9709.
- (19) Firouzi, A.; Kumar, D.; Bull, L. M.; Bessier, T.; Sieger, P.; Huo, Q.; Walker, S. A.; Zasadinski, J. A.; Glinka, C.; Nicol, J.; Margolese, D.; Stucky, G. D.; Chmelka, B. F. *Science* **1995**, 267, 1138.
- (20) Monnier, A.; Schüth, F.; Huo, Q.; Kumar, D.; Margolese, D.; Maxwell, R. S.; Stucky, G. D.; Krishnamurthy, M.; Petroff, P.; Firouzi, A.; Janzationicke, M.; Chmelka, B. F. *Science* **1993**, 1261, 1299.
- (21) Regev, O. *Langmuir* **1996**, 12, 4940.
- (22) Zholobenko, V. L.; Holmes, S. M.; Cundy, C. S.; Dwyer, J. *Microporous Mater.* **1997**, 11, 83.
- (23) Ortlam, A.; Rathousky, J.; Schulz-Ekloff, G.; Zukal, A. *Microporous Mater.* **1996**, 6, 171.
- (24) Zhang, J.; Luz, Z.; Goldfarb, D. *J. Phys. Chem. B* **1997**, 101, 7087.
- (25) Zang, J.; Carl, P. J.; Zimmermann, H.; Goldfarb, D. *J. Phys. Chem.* **2002**, 106, 5382.
- (26) Galarneau, A.; Di Renzo, F.; Fajula, F.; Mollo, L.; Fubini, F.; Ottaviani, M. F. *J. Colloid Interface Sci.* **1998**, 201, 105.
- (27) Ottaviani, M. F.; Galarneau, A.; Desplandier-Giscard, D.; Di Renzo, F.; Fajula, F. *Microporous Mesoporous Mater.* **2001**, 44, 1.
- (28) Ottaviani, M. F.; Moscatelli, A.; Desplandier-Giscard, D.; Di Renzo, F.; Kooyman, P. J.; Alonso, B.; Galarneau, A. *J. Phys. Chem. B* **2004**, 108, 12123.
- (29) (a) Martini, G.; Ottaviani, M. F.; Romanelli, M. J. *Coll. Interface Sci.* **1983**, 94, 107. (b) Romanelli, M.; Ottaviani, M. F.; Martini, G. *J. Coll. Interface Sci.* **1983**, 96, 373. (c) Martini, G.; Bindi, M.; Ottaviani, M. F.; Romanelli, M. J. *Colloid Interface Sci.* **1985**, 107, 140, 108. (d) Martini, G.; Ottaviani, M. F.; Romanelli, M.; Kevan, L. *Colloid Surf.* **1989**, 41, 149.
- (30) (a) Ottaviani, M. F.; Mollo, L.; Fubini, B. *J. Colloid Interface Sci.* **1997**, 191, 154. (b) Ottaviani, M. F.; Tomatis, M.; Fubini, B. *J. Colloid Interface Sci.* **2000**, 224, 169.
- (31) (a) Schneider, D. J.; Freed, J. H. in *Biological Magnetic Resonance. Spin Labeling. Theory and Applications*; Berliner, L. J., Reuben, J., Eds.; Plenum Press: New York, 1989, Vol. 8, p. 1. (b) Budil, D. E.; Lee, S.; Saxena, S.; Freed, J. H. *J. Magn. Res. A* **1996**, 120, 155.
- (32) Galarneau, A.; Desplandier-Giscard, D.; Dutartre, R.; Di Renzo, F. *Microporous Mesoporous Mater.* **1999**, 27, 297.
- (33) Ottaviani, M. F.; Favuzza, P.; Sacchi, B.; Turro, N. J.; Jockusch, S.; Tomalia, D. A. *Langmuir* **2002**, 18, 2347.
- (34) Tanford, C. *The Hydrophobic Effect*; Gordon and Breach Science Publishers: New York, 1980.